AJNR Am J Neuroradiol 26:711–718, April 2005

Preangiographic Evaluation of Spinal Dural Arteriovenous Fistulas with Elliptic Centric Contrast-Enhanced MR Angiography and Effect on Radiation Dose and Volume of Iodinated Contrast Material

Patrick H. Luetmer, John I. Lane, Julie R. Gilbertson, Matt A. Bernstein, John Huston III, and John L. D. Atkinson

BACKGROUND AND PURPOSE: **The detection and localization of spinal dural arteriovenous fistulas (AVFs) remain diagnostic challenges. This study tested the hypothesis that elliptic centric contrast-enhanced MR angiography (MRA) can be used to detect spinal dural AVFs, predict the level of fistulas, and reduce the radiation dose and volume of iodinated contrast material associated with conventional angiography.**

METHODS: **We examined 31 patients who presented with suspected spinal dural AVF between December 2000 and March 2004. All patients underwent MRA and conventional angiography. The effect of MRA on subsequent conventional angiography was assessed by analyzing total fluoroscopy time and volume of iodinated contrast material used.**

RESULTS: **At angiography, spinal dural AVFs were diagnosed in 22 of 31 patients, and MRA depicted an AVF in 20 of the 22 patients. MRA findings correctly predicted a negative angiogram in seven of nine cases. Of the 20 true-positive MRA results, the level of the fistula was included in the imaging volume in 14. In 13 of these 14 cases, MRA results correctly predicted the side and the level of the fistula to within one vertebral level. Fluoroscopy time and the volume of contrast agent was reduced by more than 50% in the 13 patients with a spinal dural AVF in whom MRA prospectively indicated the correct level.**

CONCLUSION: **Contrast-enhanced MRA can be used to detect spinal dural AVFs, predict the level of fistulas, and substantially reduce the radiation dose and volume of contrast agent associated with catheter spinal angiography.**

Timely diagnosis and localization of the site of spinal dural arteriovenous fistulas (AVFs) remain diagnostic challenges despite increased recognition of the disease as a treatable cause of myelopathy. Catheter spinal angiography remains the definitive diagnostic technique, but it is invasive and associated with extensive catheter manipulation, high radiation doses, and large volumes of iodinated contrast material. Selecting patients appropriately and limiting the radiation exposure and volume of contrast agent during conventional angiography are critical to optimal patient care. Contrast-enhanced MR angiography (MRA) is sensitive and specific in detecting spinal dural AVFs and can be used to predict the location of the fistulas (1–2). This study was conducted to test the hypothesis that elliptic centric contrast-enhanced MRA can be used to detect spinal dural AVFs and predict the level of fistulas and also reduce the radiation dose and volume of iodinated contrast material associated with subsequent confirmatory conventional angiography.

Received May 28, 2004; accepted after revision August 31.

From the Departments of Radiology (P.H.L., J.I.L., J.R.G., M.A.B., J.H.) and Neurosurgery (J.L.D.A.), Mayo Clinic, Rochester, MN.

Supported in part by NIH Grant EB00212.

Patrick H. Luetmer, MD, Department of Radiology, Mayo Clinic, 200 First St SW, Rochester, MN 55095.

© American Society of Neuroradiology

Methods

Institutional review board approval was obtained before the study. All involved patients gave informed consent for their participation in this research.

Patient Population

Between December 2000 and March 2004, 31 patients were referred for catheter spinal angiography for evaluation of a

spinal dural AVF, which was suspected on the basis of combined findings from spinal MR imaging and clinical findings of myelopathy. MR imaging of the entire spine without and with gadolinium enhancement had been performed in all cases. MRA with a bolus administration of gadolinium-based contrast agent had been performed in 25 patients as part of the clinical evaluation before their referral for spinal angiography. The remaining six patients underwent MRA at the time of spinal angiography. The interval from MRA to conventional angiography ranged from several hours to 27 days, with mean of 4 days.

MR Imaging

Gadolinium-enhanced, elliptic centric–ordered, 3D MRA was preformed on a four-channel cervical-thoracic-lumbar spine array coil by using the following parameters: 28 × 19.6-cm FOV, 44 1.4 mm sections yielding a 6.2-cm slab, 45° flip angle, 256 × 224 matrix, one signal acquired, and an imaging time of 49 seconds resulting in an acquisition voxel size of 1.09 × 1.25 × 1.4 mm and a voxel volume of 1.91 mm^3. Reconstruction was performed with zero-filling in all three directions, which yielded 88 sections 1.4 mm thick, with a 0.7-mm overlap and a 512 × 512 matrix. For the first 10 patients, a single acquisition was obtained in the oblique coronal plane. The image volume was centered to cover the spinal canal with superior-inferior center at T12 unless results of previous MR imaging suggested a different level. To prevent the repeated difficulty of fistulas located outside of the image volume, for the last 21 patients, two overlapping sagittal acquisitions were obtained and the FOV was increased to 32 × 22.4 cm, which allowed reliable coverage of the spinal canal from C2 to S1. The cephalic acquisition was obtained first to minimize artifact associated with the prominent cervical epidural venous plexus. For this, 25 mL of 0.5 mmol/mL gadolinium-based contrast agent was injected at a rate of 3 mL/second followed by 25 mL of saline at 2 mL/s for each injection by using a dual-chamber power injector. The imaging delay was based on the circulation time measured at the lower thoracic aorta after the injection of 2 mL of contrast agent at a rate of 3 mL/s followed by 25 mL of saline at 2 mL/s. For the first 10 patients, radial maximum intensity projection (MIP) images were created; these were tightly cropped about the axis formed by the central spinal canal. For the last 21 patients, sagittal and coronal, thin (6-mm) MIP images were created at 2-mm increments through the spinal canal. The source images were transferred to an independent workstation, which allowed for 3D reformatting and review by one of several neuroradiologists (PHL, JIL, JRG, JH) performing the clinical interpretations.

MR imaging examinations were performed by using a 1.5-T clinical machine, and all examinations included at least sagittal T1-weighted (TR/TE/NEX = 400–535/14–18/3, FOV = 22–32) sequences without and with gadolinium enhancement, as well as fast spin-echo T2-weighted (TR/TE/NEX = 3250–3350/102–105/4, FOV = 22–32) sequences.

Catheter Angiography

Small–focal spot spinal digital subtraction angiography was performed in all patients. The angiographic technique generally included selective manual injections of 3–5 mL of 300-mg/mL iodinated nonionic contrast agent into all segmental arteries from the supreme intercostal artery to the median sacral arteries with anteroposterior imaging at a rate of 2–4 frames per second. A pigtail aortogram was occasionally obtained by using 45–60 mL of 300-mg/mL iodinated nonionic contrast agent injected at a rate of 25–30 mL/s, with anteroposterior imaging over the lower spine and pelvis, as were selective series of the hypogastric branches. Repeated manual injections of 5–7 mL of contrast material with prolonged imaging up to 30 seconds were made at the levels that supply the fistula and the anterior and posterior spinal arteries. If the site of the fistula was not identified, additional injections were made into the bilateral vertebral, subclavian, costocervical, thyrocervical, and carotid arteries by using an appropriate dose and rate, with imaging over the cervical and upper thoracic spine. Complete spinal angiography occasionally required two, and in rare cases three, sessions on consecutive days because of limitations on the dosage of iodinated contrast material.

When results of preangiographic MRA suggested the location of the fistula, selective manual injections were performed at this level first. If the fistula was identified, the contralateral segmental artery and the segmental arteries one level above and one level below the fistula were studied to ensure complete evaluation of the fistula and the adjacent vasculature.

Image Analysis

In all cases, contrast-enhanced MR images, including radiographic interpretations, were available to the angiographer. MRA and radiographic interpretations were available on an independent workstation that allowed 3D reformatting of the source images at the time of conventional angiography in 19 of 31 patients. In 10 of the first 12 patients, MRAs were available without radiographic interpretation. In the remaining two, MRA was performed after catheter angiography.

For the 19 patients in whom prospective radiographic interpretation of the MRA was available, one of several neuroradiologists provided the radiographic report during a routine clinical interpretative session. Specific MRA criteria were not used, rather, the AVF was diagnosed on the basis of the interpreting neuroradiologists' perception of the size, number, and tortuousity of the intradural medullary veins and coronal venous plexus. The report specified whether the MRA was positive or negative for a spinal dural AVF. If the MRA was positive for an AVF, the report indicated the side and neural foraminal level of the suspected fistula or indicated that the level was indeterminate. For the first 12 patients, who were examined when spinal MRA was being introduced into clinical practice, a clinical radiographic interpretation was not provided before angiography. For these patients, an experienced neuroradiologist (JRG) who was blinded to the results of the catheter angiograms and who reviewed the MRA source images and MIPs on an independent workstation (which allowed 3D reformatting of the source images) provided a retrospective interpretation of the MRA. The MRA were presented in a random fashion. AVF was diagnosed on the basis of the neuroradiologist's perception of the size, number and tortuousity of the intradural medullary veins and coronal venous plexus. For each case, the reviewer completed a form with two questions: Is a fistula present in this patient? If yes, what is the side and neural foraminal level of the fistula or is the level indeterminate?

A second experienced neuroradiologist (PHL) reviewed the contrast-enhanced MR images and catheter spinal angiograms. For all patients, the catheter angiograms were evaluated for the presence and location of a fistula. T2-weighted MR images were evaluated for increased signal intensity in the spinal cord and extension of signal abnormality to the conus, and T1- and/or T2-weighted images were evaluated for flow voids or scalloping of the posterior aspect of the cord. Also assessed were mass effect, pathologic enhancement of the coronal venous plexus, and parenchymal enhancement.

Catheter Angiography Dose Analysis

To determine whether preangiographic MRA reduced the radiation exposure or volume of contrast agent associated with subsequent conventional angiography, we recorded the total fluoroscopy time and the total volume of 300-mg/mL iodinated nonionic contrast material. The patients were divided into three groups. Group A included patients in whom MRA correctly depicted the side and level of the AVF and in whom MRA images were available to the angiographer before catheter angiography. Group B included patients in whom the catheter angiogram confirmed the AVF, but MRA was per-

formed after conventional angiography or MRA did not localize the AVF. Group C included all patients with a negative catheter angiogram.

Results

Diagnosis of Spinal Dural AVF

Spinal dural AVFs were confirmed at conventional angiography in 22 of 31 patients and were excluded in the remaining nine. MRA depicted the AVF in 20 of 22 positive cases, with a sensitivity of 91%. MRA results were correctly predictive of a negative conventional angiogram in seven of nine cases, with specificity of 78%. In two false-positive MRA, normal vessels were misinterpreted as being pathologically prominent. One of the false-negative results occurred in a patient who had a subtle, slow-flow spinal dural AVF with an equivocal catheter angiogram, which led to surgical exploration, during which an AVF was confirmed. MRA provided additional support for the noninvasive diagnosis of a spinal dural AVF, particularly in three cases where spin-echo images demonstrated little to no evidence of abnormal flow voids along the surface of the spinal cord.

MR imaging findings of spinal dural AVF included increased T2 signal intensity in the spinal cord, which was noted in 19 of 22 patients with a spinal dural AVF and six of nine patients without an AVF. Three patients with an AVF had equivocal or no signal intensity in the spinal cord on T2-weighted images. Images in none of these patients demonstrated contrast enhancement of the cord parenchyma. Two of the three had definite prominent vessels on the surface of the cord, as noted on T2-weighted and gadolinium-enhanced images. Both patients also had positive MRAs, with the fistula correctly localized in one and the fistula outside of the FOV in the other. The other patient without abnormal signal intensity on T2-weighted images had subtle prominent vessels on gadolinium-enhanced T1-weighted images but had a false-negative MRA. The typical combination of increased signal intensity on T2-weighted images with contrast enhancement in the cord parenchyma and prominent vessels on the surface of the cord (Figs 1 and 2) was observed in 14 patients with a spinal dural AVF and in one patient without an AVF.

Localization of Spinal Dural AVF

On the 20 true-positive MRAs, the level of the fistula was included in the imaging volume in 14 cases. In 13, MRA results correctly predicted side and level of the fistula to within one vertebral level. Five of the six cases in which the fistula was located outside the imaging volume occurred in the first 10 patients, for whom a single coronal acquisition was used. In the last 21 patients, only one fistula occurred outside the imaging volume in the sacrum.

Reduction in Extent of Catheter Angiography

Because of limits on the volume of iodinated contrast material, two-stage angiography was required in two patients, and three-stage angiography were required in two to identify the site of fistula. In three of these patients, MRA results were positive, but the site of the fistula was outside the FOV, with one fistula located at T5 and two in the sacrum. These three cases occurred before we switched the MRA technique to the double sagittal acquisition. The fourth patient required two-stage angiography despite correct localization of a slow flow fistula to T6. Two of the nine negative angiograms required two stages, and one required three stages to complete the evaluation of the craniospinal vasculature.

To determine the effect of MRA on radiation exposure and volume of iodinated contrast agent, the patients were pooled into three groups. Group A included 13 patients, in whom MRA was performed before angiography and correctly depicted the side and level of the AVF. Group B included nine patients in whom catheter angiography confirmed the AVF but the MRA did not help in targeting catheter angiography. Of these patients, MRA was performed after catheter angiography in two, MRAs were falsely negative in two, the level was incorrect in one, and the fistula was outside the FOV in four. In nine patients in group C, no AVF was identified after complete catheter spinal angiography. Two had false-positive MRAs. The Table shows the average fluoroscopy times and volumes of contrast agent.

Localization of the spinal dural AVF with MRA before conventional angiography was associated with a >50% reduction in the fluoroscopy time and volume of iodinated contrast agent compared with cases in which MRA was performed after conventional angiography or in which MRA did not localize the fistula. Complete negative spinal catheter angiograms required relatively large volumes of contrast agent and long fluoroscopy time regardless of whether preprocedural MRAs were positive or negative.

Discussion

Spinal dural AVFs, or type I arteriovenous malformations in the Anson and Spetzler classification (3), are the most common form of spinal vascular malformation and are a potentially reversible causes of myelopathy (3–5). Venous hypertension is now recognized to cause symptoms (6–8). Microvascular studies have shown that the lesions are complex, transdural microfistulas rather than true arteriovenous malformations (9). The fistulas are typically located along the dura of a proximal root sleeve and drain to one medullary vein, with retrograde flow to the coronal venous plexus. The fistulas are small and difficult to visualize directly. Their MR imaging appearance is secondary to effects of venous hypertension in the dilated venous outflow tract. Increased signal intensity in the cord on T2-weighted images is present in nearly all cases. The increased T2 signal intensity is typically homogenous and central, sparing a thin rim of the cord peripherally and often extending to the conus. Mild cord enlargement, parenchymal gadolinium enhancement, and enhancement and

FIG 1. Images in a 53-year-old woman with a 3-year history of progressive, burning pain; numbness; and subsequent weakness in her lower extremity. She had bladder incontinence in the last year. *Left*, Sagittal fast spin-echo image shows increased T2 signal intensity and mild swelling involving the lower cord and conus. Flow voids are present over the dorsal surface of the cord. *Middle* and *right*, Sagittal T1-weighted images without (*middle*) and with (*right*) gadolinium enhancement show patchy enhancement of the lower cord and conus. It is difficult to appreciate the prominent coronal venous plexus on the enhanced image.

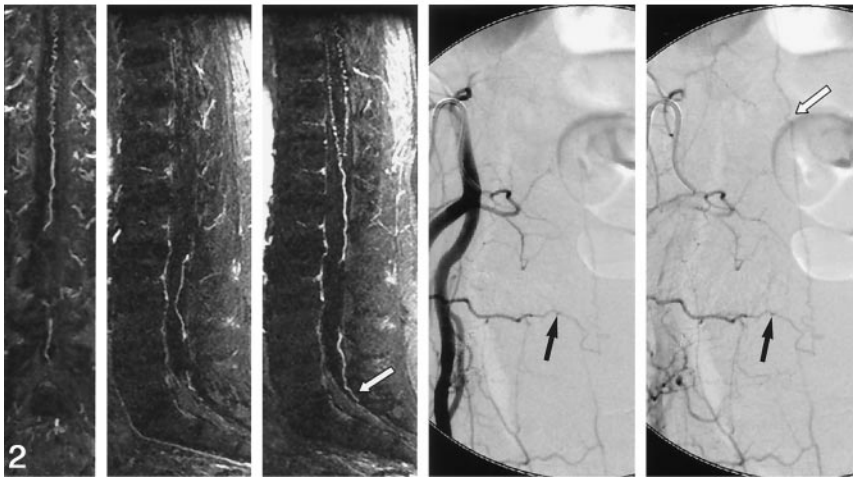

FIG 2. Sagittal MRA performed with a bolus of gadolinium-based contrast agent. Thin, 6-mm coronal (*far left*) and sagittal (*middle left* and *middle*) MIP images obtained at 2-mm increments through the spinal canal show a prominent, tortuous medullary vein extending from the level of the lower body of S1 (*white arrow*) to the conus and a dilated coronal venous plexus. Catheter, right internal iliac angiograms (*middle right* and *right*) show a spinal dural AVF at S4 on the right (*black arrows*). Draining medullary vein is relatively straight until it begins to meander in the subarachnoid space at the level of the lower body of S1 (*white arrow*).

Dose correlation with localization of AVF before catheter angiography

Group	Fluoroscopy Time (min)	Dose of Iodinated Contrast Agent (mL)
A, MRA localized AVF before angiography (n = 13)	26.3	146
B, MRA did not localize AVF before angiography (n = 9)	55.1	325
C, No spinal dural AVF found despite angiography (n = 9)	50.3	288

flow voids in tortuous vessels along the dorsal surface of the cord are typically seen (4).

Spinal dural AVF remain a diagnostic challenge despite increased recognition of the disease as a treatable cause of myelopathy and despite improvements in diagnostic imaging techniques. Atkinson and colleagues (10) reported a series of 94 patients with spinal dural AVF treated between June 1985 and December 1999. In this population, the average delay from symptom onset to diagnosis was 23 months, with a range of 2–120 months. Although 93 patients had some postoperative improvement, as shown by using a modified Aminoff-Logue scale, older patients with severe long-term deficits had poor outcomes. Westphal and Koch (11) reported a similar experience in 47 patients treated between 1991 and 1999, with mean

interval of 2 years between symptom onset and diagnosis. The degree of recovery was correlated with the severity and duration of symptoms. Lev et al reported (12) nine patients treated in 1998–1999 with a duration of symptoms before diagnosis of 6–36 months.

Prompt recognition and treatment are vital to preserving spinal cord function. The typical patient is aged 40–80 years and presents with gradual onset of slowly progressive or stepwise worsening myelopathy characterized by lower-extremity weakness, sensory loss to pinprick and light touch, and late development of bowel and bladder dysfunction (10). Most patients are referred to MR for myelopathy, and nearly all patients have T2 signal intensity abnormality in the lower thoracic cord and conus (4). This finding may be missed, and spinal stenosis may be misdiagnosed. Patients may be referred after undergoing one or more unsuccessful decompressive lumbar laminectomy procedures (10–12). Alternatively, the signal intensity of the spinal cord may be identified but misinterpreted as transverse myelitis, medullary infarct, or spinal cord tumor (10–11). Biopsy of the cord is unnecessary and may also lead to an erroneous histologic conclusion of glioma if the reactive gliosis is misinterpreted as tumor (11).

A critical juncture in the evaluation of patients with spinal dural AVF occurs at the time of their first referral for spinal MR study. The radiologist must have a high degree of suspicion and recognize the MR features of spinal dural AVF. Once the diagnosis is considered, MRA can play a valuable role in confirming the diagnosis and targeting conventional catheter angiography.

In this study, 86% of patients with spinal dural AVF had definite abnormal T2 signal intensity in the spinal cord. This finding was sensitive for spinal dural AVF but not specific, and it was seen in 67% of patients who did not have an AVF. The presence of hazy parenchymal contrast enhancement and prominent vessels on the surface of the cord on spin-echo images increased the specificity of the MR findings, but this in combination with abnormal T2 signal intensity was present in only 64% of our patients with a spinal dural AVF (Figs 1 and 2).

Spinal MRA is an attractive tool for increasing the sensitivity and specificity of the MR examination. Over the past decade, multiple spinal MRA techniques have been developed. Early efforts included 2D (13–14) and 3D (15–16) phase-contrast techniques. In 1995, Bowen et al (17) reported application of an 11 minute contrast-enhanced 3D time of flight sequence with high spatial resolution. Eight patients with spinal dural AVFs were examined, and the pathologic intradural vessels were identified in all eight. The level of the draining medullary vein was identified in six. Using a similar technique in 2002, Saraf-Lavi et al (1) reported a larger series of 21 patients with spinal dural AVF and 11 control subjects. In this study, three reviewers who were blinded to the final diagnosis achieved sensitivities and specificities for dural fistulas of 80%–100% and 82%, respectively, when the MR images and MRAs were analyzed together. On average, the percentage of true-positive results for which the correct fistula level was predicted was 50%, and the correct level ± one level was 73%.

In 2002, Farb et al (2) reported nine patients examined by using an autotriggered, elliptic centric–ordered, 3D gadolinium-enhanced technique. The images were acquired in the sagittal plane by using a 36 × 27 FOV and achieved high spatial resolution with nearly isotropic voxel dimensions of 1.0 × 1.0 × 1.2 mm in 118 seconds. Abnormal intradural vessels were identified in all patients, and the level of fistula was correctly prospectively identified in eight of nine.

The use of elliptic centric–ordered 3D technique combined with a rapid bolus injection and a robust timing mechanism is a technical advance in spinal MRA for the evaluation of spinal dural AVFs. The technique provides high spatial resolution despite a relatively short imaging time. T1-weighted short-TR imaging with elliptic centric–ordered filling of k-space results in a final image on which the signal intensity of the structures are determined on the basis of the state of gadolinium enhancement during the first several seconds of the sequence (18). This has the effect of maximizing the intravascular contrast relative to background contrast. In our series, the bolus of contrast agent was timed to maximize contrast within the arterialized intradural draining medullary vein and the coronal venous plexus rather than the fistulas, which were much smaller and more difficult to visualize. Spinal dural AVF was diagnosed on the basis of the neuroradiologist's perception of the size, number, and tortuousity of the intradural vessels rather than on specific criteria for these imaging features or on the direct visualization of the fistulas. This approach is similar to the method of analysis Saraf-Lavi et al (1) performed, and we achieved essentially equivalent sensitivity and specificity.

During this study, we realized that two overlapping acquisitions were required to adequately cover the spinal canal. Acquisition in the sagittal rather than coronal plane improved the ability to include all of the spinal canal, especially in patients with kyphosis. Studying the cervical and upper thoracic canal with the first bolus of gadolinium contrast agent is preferred, since the prominent epidural venous plexus in the cervical canal can result in artifact if the cervical region is studied with the second bolus. We noted a substantial improvement in the ability to localize the fistula in the last 21 patients, in whom overlapping sagittal acquisitions were obtained. Only one sacral fistula occurred outside the imaging volume in these patients. A notable advantage of the elliptic centric technique was the short 49-second imaging time, which allowed routine acquisition of two overlapping series with good patient acceptance and minimal patient motion.

We also found that an imaging workstation, which allowed rapid review of source images as well as 3D analysis of the image data set, was helpful for interpreting MRAs (Fig 3). We found that thin, sagittal and coronal MIP images were more helpful than

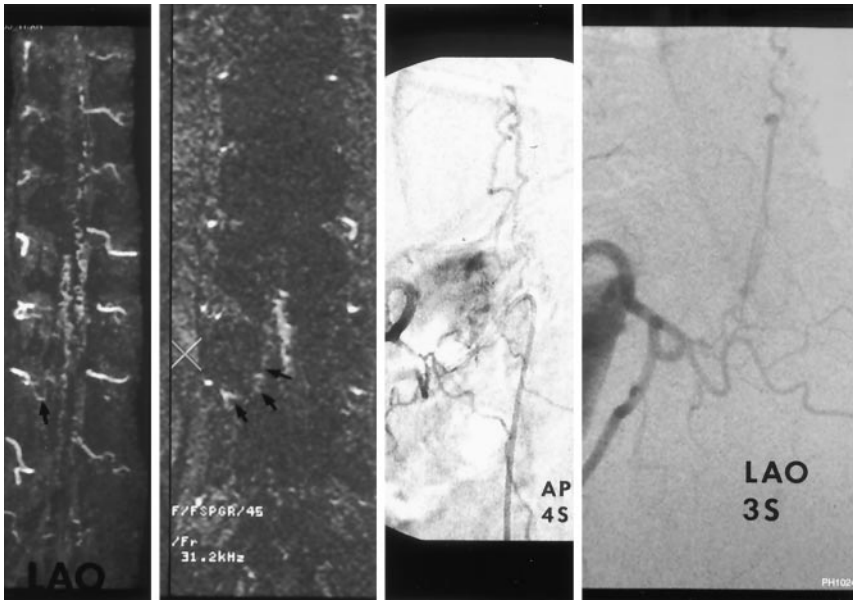

FIG 3. Images in a 72-year-old man with a 2-year history of urinary incontinence with progressive perianal and lower-extremity numbness and loss of lower-extremity control over the last year leading to use of a wheelchair in the last 2 months. *Far left*, MIP image in the left anterior oblique projection shows prominent, tortuous vessels on the dorsal and ventral surfaces of the cord and a prominent vessel extending from the right T11 foramen (*arrow*). *Middle left*, Source image confirms a prominent vessel (*arrows*) extending from below the right T11 pedicle (*X*) to prominent vessels on the surface of the cord. *Middle right* and *right*, Catheter angiograms in anteroposterior and left anterior oblique views at T11 on the right confirms a spinal dural AVF inferior to the right T11 pedicle draining to a dilated coronal venous plexus.

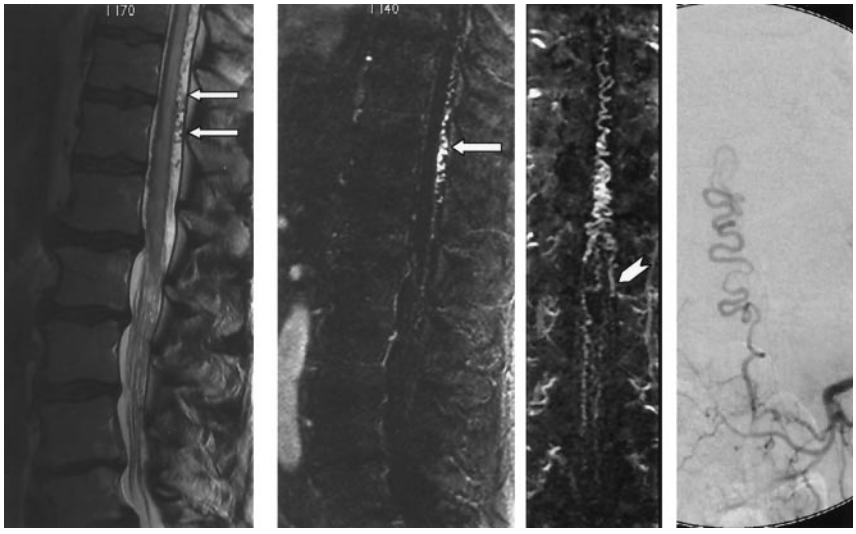

FIG 4. Images in a 64-year-old man with a 13-month history of progressive lower trunk and lower-extremity numbness and mild bowel and bladder urgency. *Far left*, Sagittal T2-weighted fast spin-echo image shows increased T2 signal intensity and mild swelling involving the lower spinal cord and conus, with prominent flow voids over the dorsal surface of the cord (*arrows*). *Middle left* and *middle right*, MRA performed with a bolus of gadolinium-based contrast agent. Thin, 6-mm sagittal (*middle left*) and coronal (*middle right*) MIP images at 2 mm increments through the spinal canal confirm a dilated coronal venous plexus along the dorsal surface of the cord (*arrow*) and show a prominent medullary vein extending from the left L1 foramen (*arrowhead*). *Far right*, Catheter angiogram confirms a spinal dural AVF at L1 on the left side.

radial MIP images tightly collimated to the central spinal canal (Fig 4s and 5). We now include sagittal and coronal, thin (6-mm) MIP images at 2-mm increments as standard reformatted views for image review and archiving.

Ideally, the elliptic centric–ordered technique would allow direct visualization of the fistula. However, at this time, we have not been successful in developing a sequence that can reliably demonstrate the actual fistula or resolve arterial and venous phases with differential enhancement of the fistula and draining medullary vein compared with the engorged coronal venous plexus. In this study, the level of the fistula was indirectly inferred by tracing an engorged medullary vein from the coronal venous plexus back to the level of a neural foramen. Therefore, an important drawback of this technique is the apparent inability to distinguish medullary veins that drain from the dural AVF toward the coronal venous plexus from those that provide egress from the coronal venous plexus. In several cases, the tortuous medullary vein draining the dural AVF approached a neural foramen above the level of the AVF, resulting in false localization (Fig 5).

Further refinement of spinal MRA is desired. Utilization of 3.0-T systems and eight-channel coils could provide increased signal-to-noise ratios. Techniques such as parallel imaging could then be utilized to decrease imaging times without sacrificing spatial resolution. This may yield time-resolved images that allow sequential visualization of the feeding arteries, fistula, draining medullary vein, and engorged coronal venous plexus.

Our results confirm the previously documented sensitivity and specificity of MRA and the usefulness of MRA in predicting the level of spinal dural AVF (1–2), and our experience confirms that these results can be achieved during busy, routine, clinical readout sessions. In addition, the value of MRA as a planning tool for conventional angiography was demonstrated. Preangiographic MRA localization of the fistula was associated with a dramatic reduction in fluoroscopy

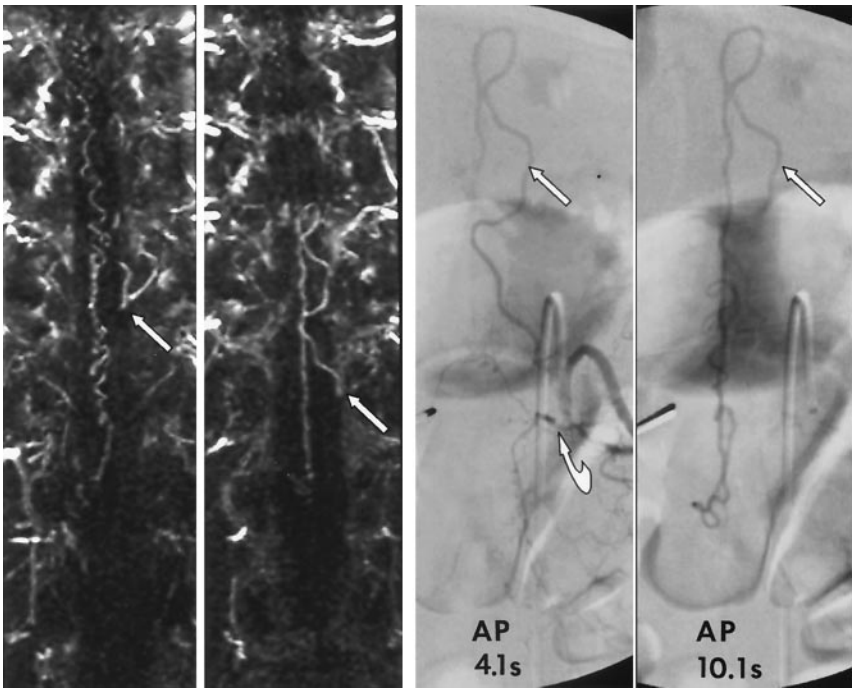

FIG 5. Images in a 62-year-old man with a 19-month history of progressive lower-extremity motor and sensory dysfunction and neurogenic bladder diagnosed elsewhere, with transverse myelitis. *Far left* and *middle left*, MRA performed with a bolus of gadolinium-based contrast agent and thin, 6-mm coronal MIP images obtained at 2-mm increments through the spinal canal. *Far left*, Image shows a prominent medullary vein at the level of the left T11 foramen (*arrow*). *Middle left*, Image shows that the medullary vein is continuous with a prominent medullary vein emanating from the left T12 foramen (*arrow*). *Far right* and *middle right*, Limited catheter, 4- and 10-second spinal angiograms confirm a spinal dural AVF located under the left T12 pedicle (*curved arrow*). Left T12 medullary vein loops back toward the left T11 foramen (*straight arrow*). The 10-second delayed image shows opacification of the dilated coronal venous plexus. MRA allowed us to limit angiography to the bilateral T11-L1 segmental arteries and thus limit the cost, radiation exposure, and dose of contrast agent (to 57 mL).

time and volume of contrast agent. Reduced fluoroscopy time implies a reduction in catheter manipulation and total procedural time. It is logical to postulate that reductions in fluoroscopy time, total procedural time, and catheter manipulation are associated with reduced risk of complications. However, this potential is difficult to prove given the low reported complication rate for spinal angiography (19), the absence of notable angiographic complications in the patient cohorts in this study, and the relatively small numbers of patients. The risk of ionizing radiation is also low and difficult to quantitate. However, the policy of the Nuclear Regulatory Commission to keep radiation doses as low as reasonably achievable (ie, ALARA) (20) affirms the value of reducing radiation doses.

Likewise, it was not possible to demonstrate a difference in patient outcome due to the reduction in contrast volume achieved in this small patient population. However, it is reasonable to postulate that the already low risk of contrast medium–induced nephrotoxicity can be further minimized by utilizing MRA as a preangiographic planning tool, given the approximately 50% reduction in volume of contrast agent achieved in this study. Reduction in the number of spinal levels examined also substantially reduces the cost of conventional angiography.

Conclusion

Despite limitations in the technique used in the current study, we demonstrated that contrast-enhanced MRA can be used to detect spinal dural AVFs, predict the level of fistulas, and substantially reduce the radiation dose and volume of iodinated contrast material associated with catheter spinal angiography. We advocate performing MRA in all patients in whom clinical examination or MR imaging results suggest a fistula. In our practice, MRA has replaced prone-supine CT myelography in determining the presence of a spinal dural AVF before conventional angiography. Utilization of elliptic centric contrast-enhanced MRA, which is available on most commercial MR machines, along with recognition of the MR imaging features of spinal dural AVF, provide the opportunity to reduce the delay in diagnosis and improve the efficiency of characterizing this reversible cause of myelopathy.

References

1. Saraf-Lavi E, Bowen BC, Quencer RM, et al. **Detection of spinal dural arteriovenous fistulae with MR imaging and contrast-enhanced MR angiography: sensitivity, specificity, and prediction of vertebral level.** *AJNR Am J Neuroradiol* 2002;23:858–867
2. Farb RI, Kim JK, Willinsky RA, et al. **Spinal dural arteriovenous fistula localization with a technique of first-pass gadolinium-enhanced MR angiography: initial experience.** *Radiology* 2002;222:843–850
3. Anson JA, Spetzler RF. **Classification of spinal arteriovenous malformations and implications for treatment.** *BNI Qtr* 1992;8:2–8
4. Gilbertson JR, Miller GM, Goldman MS, Marsh WR. **Spinal dural arteriovenous fistulas: MR and myelographic findings.** *AJNR Am J Neuroradiol* 1995;16:2049–2057
5. Grote EH, Bien S. **Arteriovenous malformations of the spinal cord.** In: Youmans JR, ed. *Neurological Surgery*. 4th ed. Philadelphia: W.B. Saunders; 1996:1511–1530
6. Criscuolo GR, Oldfield EH, Doppman JL. **Reversible acute and subacute myelopathy in patients with dural arteriovenous fistulas: Foix-Alajouanine syndrome reconsidered.** *J Neurosurg* 1989;70:354–359
7. Hurst RW, Kenyon LC, Lavi E, Raps EC, Marcotte P. **Spinal dural arteriovenous fistula: the pathology of venous hypertensive myelopathy.** *Neurology* 1995;45:1309–1313
8. Kataoka H, Miyamoto S, Nagata I, Ueba T, Hashimoto N. **Venous congestion is a major cause of neurological deterioration in spinal arteriovenous malformations.** *Neurosurgery* 2001;48:1224–1230
9. McCutcheon IE, Doppman JL, Oldfield EH. **Microvascular anatomy of dural arteriovenous abnormalities of the spine: a microangiographic study.** *J Neurosurg* 1996;84:215–220

10. Atkinson JLD, Miller GM, Krauss WE, et al. **Clinical and radiographic features of dural arteriovenous fistula, a treatable cause of myelopathy.** *Mayo Clin Proc* 2001;76:1120–1130
11. Westphal M, Koch C. **Management of spinal dural arteriovenous fistulae using an interdisciplinary neuroradiological/neurosurgical approach: experience with 47 cases.** *Neurosurgery* 1999;45:451–458
12. Lev N, Maimon S, Rappaport ZH, Melamed E. **Spinal dural arteriovenous fistulae: a diagnostic challenge.** *Israel Med Assoc J Imag* 2001;3:492–496
13. Gelbert F, Guichard JP, Kourier KL, et al. **Phase-contrast MR angiography of vascular malformations of the spinal cord at 0.5 T**. *J Magn Reson Imaging* 1992;2:631–636
14. Mascalchi M, Bianchi MC, Quilici, et al. MR **Angiography of spinal vascular malformations.** *AJNR Am J Neuroradiol* 1995;16:289–297
15. Mascalchi M, Quilici N, Ferrito G, et al. **Identification of the feeding arteries of spinal vascular lesions via phase-contrast MR angiography with three-dimensional acquisition and phase display.** *AJNR Am J Neuroradiol* 1997;18:351–358
16. Provenzale JM, Tien RD, Felsbert GJ, Hacein-Bey L. **Spinal dural arteriovenous fistula: demonstration using phase contrast MRA.** *J Comput Assist Tomogr* 1994;18:811–814
17. Bowen BC, Kraser K, Kochan JP, Pattany PM, Green BA, Quencer RM. **Spinal dural arteriovenous fistulas: evaluation with MR angiography.** *AJNR Am J Neuroradiol* 1995;16:2029–2043
18. Huston J, Fain SB, Riederer SJ, Wilman AH, Bernstein MA, Busse RF. **Carotid arteries: maximizing arterial to venous contrast in fluoroscopically triggered contrast-enhanced MR angiography with elliptic centric view ordering.** *Radiology* 1999; 211: 265–273
19. Forbes G, Nichols DA, Jack CR, et al. **Complications of spinal cord arteriography: prospective assessment of risk for diagnostic procedures.** *Radiology* 1988;169:479–484
20. 10 Code of Federal Regulations Part 835, December 14, 1993, **Occupational Radiation Protection, Final Rule.** *Federal Register*; 58:238